Photocatalytic Potential of Metal-Organic Frameworks for Pollutant Degradation: A Literature Review

Syaima, Husna
Faculty of Mathematics and Natural Sciences, Mulawarman University

Meiyanti Ratna Kumalasari
Faculty of Mathematics and Natural Sciences, Palangka Raya University

Qonita Awliya Hanif
Faculty of Mathematics and Natural Sciences, Ganesha Education University

Irfan Ashari Hiyahara
Faculty of Mathematics and Natural Sciences, Mulawarman University

他

https://doi.org/10.5109/7236824

出版情報：Evergreen. 11 (3), pp.1715-1731, 2024-09. 九州大学グリーンテクノロジー研究教育センター
バージョン：

Photocatalytic Potential of Metal-Organic Frameworks for Pollutant Degradation: A Literature Review

Husna Syaima[1,*], Meiyanti Ratna Kumalasari[2], Qonita Awliya Hanif[3], Irfan Ashari Hiyahara[1], Aidilia Putri Salsabila[1], Marinda Afifatu Zahra[1]

[1]Faculty of Mathematics and Natural Sciences, Mulawarman University, Indonesia

[2]Faculty of Mathematics and Natural Sciences, Palangka Raya University, Indonesia

[3]Faculty of Mathematics and Natural Sciences, Ganesha Education University, Indonesia

*Author to whom correspondence should be addressed:

E-mail: husna.syaima@fmipa.unmul.ac.id

(Received April 1, 2024: Revised June 25, 2024: Accepted July 1, 2024).

Abstract: Photocatalysis is one of the alternatives for wastewater treatment. The photocatalytic performance of MOFs degrading dyes and other pollutants are compared in this review. Most MOFs exhibit great degradation activity, even reaching 100% dyes successfully degraded while using MIL-125(Ti) and UiO-66-NH_2@CNT types of MOFs. Factors such as pH, catalyst concentration, lighting conditions, the structure of materials, stability, and reusability, as well as techniques for characterizing MOF degradation pathways and limitation of MOFs for photodegradation, are also discussed.

Keywords: Metal-organic framework (MOFs); photodegradation; dye; pollutant, catalyst

1. Introduction

The textile industry, one of the world's largest industrial sectors, operates globally with a total revenue of $1 trillion. It constitutes 7% of the world's total exports and plays a significant role in the global economy[1)]. However, the industry is also a substantial source of environmental pollution in various countries. Fast fashion trends have contributed to worldwide apparel manufacturing and consumption during the last five decades[2,3)]. The leading cause of this problem is the inability of the textile industry to dispose of its wastewater correctly[4,5)]. This wastewater affects not only human health but also the species that live in the surrounding area, threatening the general sustainability of the environment[6,7)].

The textile industry generates many wastes, including hazardous metal components, fabric and yarn scraps, and textile dyes[8,9)]. Textile dyes, being water-soluble and highly stable to temperature, light, and other substances, present challenges in decomposition and resist removal during conventional water treatment processes[10)]. These dyes persist in the environment for extended periods without intervention[11)]. In Indonesia, the problem of water pollution has emerged as the primary focus of concern for Indonesian researchers at present[12)]. Researchers have explored many treatment options in response to the challenge of dye waste removal: mechanical, physicochemical, and biological methods[13)]. Various techniques such as adsorption, ion exchange, coagulation-flocculation, and the cutting-edge technology of advanced oxidation processes (AOPs) are also explored[14,15)]. AOPs comprise approaches such as Fenton oxidation, photo-Fenton, ozonation, electrochemical oxidation, and photocatalysis[6)].

The photocatalysis method is one of many methods in the advanced oxidation process, wherein reactive oxygen species (ROS) are generated to break down organic contaminants into non-toxic by-products[16,17)]. During the photocatalyst process, reactive oxygen species are generated, specifically hydroxyl radicals (•OH) and superoxide radicals ($O_2^{\bullet-}$), which possess powerful oxidative properties[18)]. Consequently, these radicals can be involved in chemical reactions with organic pollutants, such as dyes, forming less harmful substances[19)]. One of the materials that can be used as a catalyst in this photocatalyst process is metal-organic framework material, which can exist in pure and hybrid forms[20)].

Metal-organic frameworks (MOFs) are a recently developed group of coordination compounds that consist of metal-oxo groups and organic linkers connected through coordination interactions, leading to the formation of two- or three-dimensional skeletal structures[20,21)]. MOFs provide several benefits, including well-organized structure and clusters, high porosity, convenient modification, extensive surface area, and excellent thermal stability[22)]. Furthermore, MOFs are widely used in many chemical fields, such as separation materials, gas storage, drug delivery systems, and

catalysts[23–25] due to the flexibility of their surface structure.

MOFs have also emerged as promising materials for photocatalysis due to their tunable band gaps, which enable them to absorb light and generate electron-hole pairs necessary for photocatalytic reactions. The band gap, the energy difference between the valence band (VB) and the conduction band (CB), determines the wavelength of light that MOFs can absorb. By carefully designing the organic ligands and metal nodes in MOFs, researchers can adjust the band gap to match the energy of visible or UV light. This tunability allows MOFs to harness light energy effectively, facilitating the generation of reactive species such as hydroxyl radicals and superoxide ions, which are crucial for degrading pollutants. Among the various types of MOFs utilized for photocatalytic applications, there are several noteworthy MOFs with suitable band gaps for photocatalysis purposes (Fig. 1). Firstly, UiO-type MOFs, characterized by their robustness and large pore sizes, have shown excellent performance in photocatalytic reactions, owing to their high surface area and stability under harsh conditions. MIL-type MOFs, featuring open metal sites and tailored pore structures, also exhibit enhanced light absorption and charge separation properties, making them efficient photocatalysts for various transformations.

Moreover, with their inherent porosity and chemical stability, ZIF-type MOFs have demonstrated significant potential in photocatalytic applications, particularly in hydrogen evolution and pollutant degradation. These examples illustrate the diverse range of MOF architectures that can be tailored for photocatalysis, offering opportunities to develop advanced materials for sustainable energy and environmental remediation applications. Many other types of MOFs and composites also showed promising activity for photodegradation.

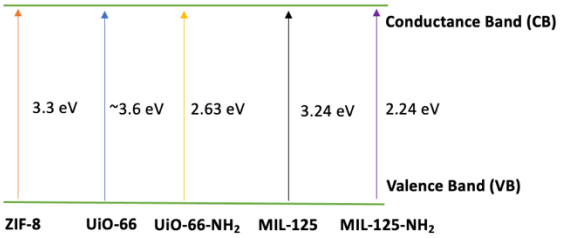

Fig. 1: Band gap of the different MOFs[26–28]

Hence, this review article will discuss the utilization of MOF materials as photocatalysts for photodegrading organic dyes and other pollutants. It will also discuss some parameters that affect their activity, challenges, and limitations of MOFs as photocatalysts.

2. Metal-Organic Frameworks

MOFs are crystalline materials constructed from inorganic metal ions or clusters linked by organic ligands through coordination interactions (Fig 2)[29,30]. The versatility of MOFs lies in the virtually limitless possibilities for tailoring their chemical properties by selecting and combining different metal ions and organic linkers. This allows for precise control over porosity and functionality, making them highly adaptable for various applications[31,32] Recently, there has been growing interest in using MOF-based materials as catalysts for thermo-, photo-, and electrocatalytic processes because of their excellent thermal stability, wide surface area and porosity, and the ability to control their acidity and basicity[25,29].

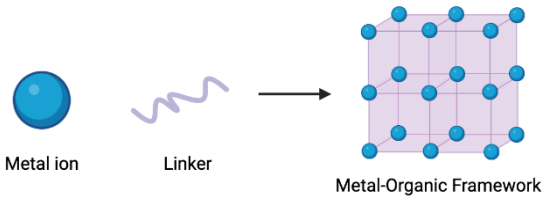

Fig. 2: Metal-organic Frameworks

Hoskin and Robson pioneered the synthesis of MOFs in the early 1990s. These materials feature a scaffold-like 3D structure constructed from octahedral/tetrahedral metal centers linked by organic ligands[21]. MOFs have attracted considerable research interest in photocatalysis due to their effectiveness as catalysts. Researchers have explored various techniques to enhance further the photocatalytic properties of pure MOFs, including metal/ligand mixture strategies, ligand functionalization, dye sensitization, and metal/ligand ion immobilization[30]. These modifications can influence charge transfer efficiency during photoexcitation, light absorption, and the subsequent utilization of absorbed energy[30,33]. Modifying the ligand orientation can impact the accessibility of the pore and ultimately determine the selectivity of MOF catalysts[32]. In addition to their pure state, MOFs can also undergo modification through composite formation with other materials, such as H_2O_2, metal, metal oxides[34], bimetallic[35], ternary metal[36], or polymetallic[37]. Enhancing its chemical and thermal stability can also influence its physiochemical characteristics, including electrical conductivity and magnetism. Composite materials consisting of MOFs and other substances promote uniform dispersion of chemical components and enhance the active surface area for catalytic activity, resulting in higher catalyst activity efficiency[31].

3. Introduction of Photocatalysis

Photocatalysis shares similarities with photochemistry, both operating on principles analogous to natural photosynthesis in plants. Both processes harness light energy to convert it into chemical forms. However, unlike photosynthesis, which employs chlorophyll, photocatalysis utilizes semiconductor materials known as "photocatalysts" to facilitate the process[38].

Photocatalysis occurs when ROS, free radicals with at least one unpaired electron, are generated. These free

radicals are crucial in breaking down pollutants with complex and large chemical structures[16,33]. During photocatalysis, electron/hole pairs are produced, resulting in the formation of hydroxyl radicals (•OH) and superoxide radicals ($O_2^{\bullet-}$), both of which possess powerful redox properties[14,39]. Photocatalysis reactions depend on only light as the exclusive energy source to activate the photocatalyst. The photocatalyst utilizes light energy to stimulate electrons in the valence band, causing them to transition to the energy band and generate photogenerated carriers[40]. This process is favorable due to its low cost, environmental friendliness, and cleanness[41]. Photocatalysis also offers several advantages for pollutant removal, including faster degradation rates, mild operating conditions[42], and tunable product selectivity[43].

In 1972, Fujishima and Honda made a significant breakthrough in photocatalysis by demonstrating that sunlight can separate water into hydrogen and oxygen using a TiO_2 electrode[39,40]. Photocatalysis can degrade organic pollutants, including dyes, using several catalysts such as metal nanoparticles, metal oxides, carbon polymers, perovskites, covalent-organic frameworks, and metal-organic frameworks[40]. The photodegradation process works by mixing photocatalytic material into polluted air and irradiating it with light[44].

4. Photocatalytic Degradation Mechanism of Pollutants by MOFs

In general, photocatalysis occurs when the catalyst is exposed to light[45]. Several electrons (e^-) will leave the valence band (*valence* band, VB) towards the conduction band (*conduction band*, CB) and leave holes (h^+) (Fig. 3). The photogenerated electrons (e^-) and holes (h^+) possess distinct chemical potentials determined by their position. Each plays a crucial role in facilitating the corresponding redox processes. Valence band vacancies, or holes (h^+), undergo a reaction with H_2O in solution, forming •OH. Similarly, electrons in the conduction band react with O_2 to produce $O_2^{\bullet-}$. The two radicals mentioned can degrade organic contaminants, specifically dyes. The byproducts of this degradation process include carbon dioxide (CO_2) and water (H_2O)[39,46–48].

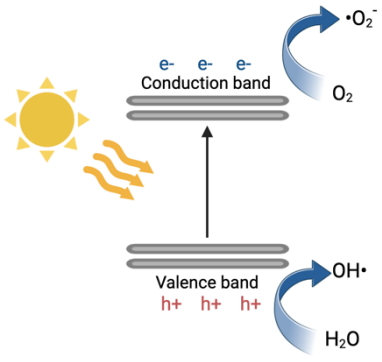

Fig. 3: Radical generation process

Based on the catalyst phase, AOPs can be categorized into heterogeneous and homogeneous photocatalysis. In heterogeneous photocatalysis, light irradiation of a semiconductor catalyst induces charge separation, producing ROS[49]. These solid-state catalysts are easily separated from the reaction mixture. However, active sites could be more frequently defined, leading to reduced initial reaction rates and the possibility of undesired byproducts. Conversely, homogenous processes suffer catalyst loss and rapid deactivation. As a result, heterogeneous photocatalysis using MOFs is a popular option for wastewater treatment due to the catalyst's reusability, which reduces costs and environmental impact. However, the accessibility of active sites inside the MOF structure can be a limiting issue, as reactant and product diffusion are slow[44].

The ability of MOFs to capture and utilize light energy is an essential factor when selecting them for photocatalysis. The highly versatile MOF framework enables precise design and modification to improve photocatalytic activity. Certain MOFs containing metal ions, such as Fe, Cr, Zr, and Ti, can successfully utilize and absorb solar energy. These MOFs frequently have a narrow bandgap, allowing them to be triggered by visible light, making them exciting candidates for the degradation of organic pollutants. Furthermore, organic linkers in MOFs enable variable light absorption and effective charge separation, resulting in longer excited state intervals in the microsecond range[44].

Mahmoodi et al. successfully synthesized MIL-100 (Fe) to degrade the textile dye basic blue 41 (BB41). This process is initiated by UV light excitation of MIL-100 (Fe), which triggers the formation of electron (e^-) and hole (h^+) pairs within the MOFs. This generation of e^-/h^+ pairs is the first step in photocatalysis. Upon light absorption, electrons are promoted from the VB to the CB, leaving behind holes in the VB (Fig. 4). These excited electrons and holes can then migrate to the MOF surface. Surface electrons reduce O_2 to $O_2^{\bullet-}$, which can further react to form •OH. Simultaneously, VB holes oxidize water molecules to generate additional •OH radicals. These highly reactive •OH are the primary species responsible for breaking down BB41 into non-toxic molecules[42].

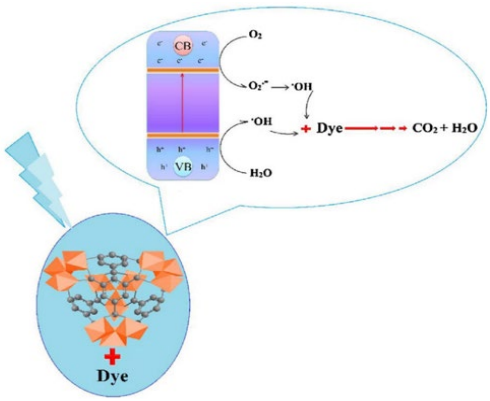

Fig. 4: Photocatalytic BB41 degradation by the MIL-100[42].

Sharma et al. used energy level diagrams to describe the photocatalytic mechanism for organic pollutant degradation in a Bi_2O_3@Fe-MOF composite[50]. Figure 5 shows that the VB and CB of Bi_2O_3 have higher positive potentials than the LUMO and HOMO of Fe-MOF. Bi_2O_3 and Fe-MOF are both excited by visible light, leading to the formation of e^- and h^+. Electrons from Bi_2O_3's conduction band move to Fe-MOF's VB due to the internal field at the heterojunction interface, triggering greater charge separation. Electrons on Fe-MOF and holes on Bi_2O_3 create reactive radicals ($O_2^{\bullet-}$ and •OH) that break down organic pollutants like rhodamine B and triclopyr.

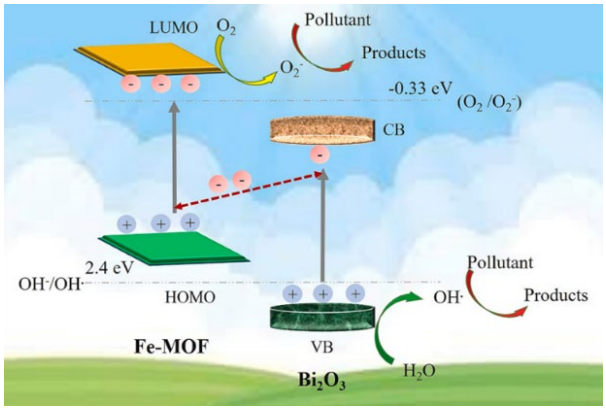

Fig. 5: Mechanism of charge transfer in Bi_2O_3@Fe-MOF for photocatalytic degradation[50]

5. Photocatalytic Degradation of Organic Dyes using MOFs

In recent decades, MOFs have shown significant promise in the photocatalytic degradation of organic pollutants. MOFs such as ZIF-8, MOF-5, MIL-125, and UiO-66 exhibit properties analogous to semiconductors, comprising metal ions and organic linkers, function akin to discrete semiconductor quantum dots equipped with light-absorbing antennae. The description of metal ions and organic linkers that construct the structures of some MOFs above can be seen in Table 1.

Table 1. Some MOFs exhibit semiconductor-like behavior.

MOFs	Empirical Formula	Metal	Linkers
MOF-5	$Zn_4O(BDC)_3$ BDC=1,4-benzene dicarboxylate	Zn	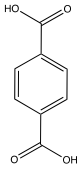
MIL-125	$Ti_8O_8(OH)_4(BDC)_6$	Ti	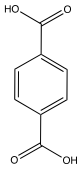
UiO-66	$(Zr_6O_4(OH)_4(BDC)_6)$	Zr	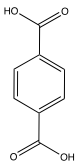
ZIF-8	Zn(2-methylimidazole)$_2$	Zn	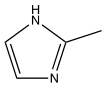

Currently, scientists are in the process of synthesizing many types of MOFs that have the potential to be utilized in the process of photocatalysis. Table 2 displays the research that uses MOFs for dye degradation. The light source utilized for the process might vary, ranging from visible, UV, and LED light to direct sunlight. The parameters employed in photocatalysis experiments differ among studies, covering factors such as the photocatalyst dosage, the reaction duration, and the type of light source used. Within the scope of this review article, the parameters of temperature and pH should be given more attention, except for a few research. The studies referenced in[51],[52], and[53] have established that the pH levels during the photocatalyst reaction were 6, 7, and 1, resulting in degradation efficiencies of 99%, 99%, and 91.70%, respectively. Regarding the temperature parameter, most of the examined studies used room temperature for the reaction. As in[54] and[55], the temperature was maintained using a water bath during the reaction process.

Regarding the results shown in Table 2, it is crucial to observe the most significant level of degradation, amounting to 100%, using MIL-125(Ti) and PCN-250(Fe_2Mn). Both individuals utilized visible light as a light source, with reaction times of 80 minutes and 290 minutes, respectively. However, the degradation efficiency of Fe-BTC[56] was also relatively low, at just 62% in 90 minutes. Both individuals utilized UV light as the light source during the photocatalysis procedure. The band gap energy is 6.63 eV.

Additionally, specific MOFs can be combined with H_2O_2 during photocatalysis to hinder the recombination of electrons and holes[51]. H_2O_2 acts as an electron inhibitor, preventing the excited electrons from returning to the valence band and reducing the number of holes generated[57]. It will enhance the production of hydroxyl radicals, increasing the degradation process's effectiveness[51]. In the previous study[58], the degradation rate was only 58% before H_2O_2 was added. However, after adding H_2O_2, the degradation rate considerably increased to 93%.

The degradation efficiency findings reported from each investigation exhibit variability. Multiple variables influence the decrease in efficiency of the photocatalysis process. The light intensity and wavelength of the light are two characteristics that have an influence[47,59]. The electron/hole recombination rate is elevated at low

intensities, impacting reactive oxygen species generation [47]. Moreover, the degradation efficiency is significantly influenced by the quantity of catalyst used[59]. The degradation efficiency will be proportionally enhanced with the amount of catalyst utilized, as this improves the number of active sites on the photocatalyst surface, amplifying the formation of •OH radicals[60]. The pH level significantly influences the degradation of pollutants during photocatalysis[47,59]. The influence of pH on the photodegradation process occurs mainly in three stages of the photocatalysis process: (1) direct oxidation by positively charged holes, (2) the activity of •OH radicals, and (3) direct reduction by electrons in the conduction band[47]. The photocatalysis process is influenced by temperature, with higher temperatures often leading to increased photocatalysis activity[59].

Nevertheless, temperatures beyond 80°C result in an elevated electron or hole collision rate[60]. Studies with degradation efficiency below 70% may overlook certain variables, such as pH and temperature, which can reduce overall degradation efficiency. Furthermore, the quantity of catalyst employed and the light intensity used throughout the reaction process may also be factors to consider.

Table 2. Different MOFs used as photocatalysts and their corresponding degradation efficiency

Materials	Dyes	Band gap (eV)	Dosage	Duration (minutes)	Light Source	Degradation (%)	Ref.
NNU-36 + H_2O_2	Rhodamine B	2.28	15 mg	60	Visible light	96.20	[61]
$Cu_3(BTC)_2$ + H_2O_2	Rhodamine B	3.68	0.5 g/L	60	Visible light	99	[51]
MIL-125(Ti)	Rhodamine B	2.70	10% wt	80	Visible light	100	[62]
Zn-BTC + H_2O_2	Rhodamine B	2.84	2 mg	90	Visible light	85	[63]
NNU-15(Ce) + H_2O_2	Rhodamine B	2.11	30 mg	12	Visible light	99	[57]
BiOBr/CAU-17-2h	Rhodamine B	2.86	-	50	Visible light	85.70	[64]
Fe_3O_4@ZnO@ZIF-8	Rhodamine B	2.58	5 mg	100	Xenon/ visible Light	98	[65]
BiOI/NH_2-MIL-125(Ti)	Rhodamine B dan p-chlorophenol	2.41	-	240	Visible light	73	[66]
Bi–Fe MOF (AGV/HBF)	Rhodamine B	2.62	-	120	Xenon light	99.40	[67]
Chitosan/MnO_2@ MOF-801	Rhodamine B	1.65	-	45	Sunlight	95	[68]
N-ZnO@NC	Methylene Blue	3.16	-	15	Visible light	50.30	[69]
Fe-BTC	Methylene blue	6.63	150 mg	90	UV light	62	[56]
$\{[Cu_2(TTB)(SO_4)(OH)]\cdot H_2O\cdot MeCN\}_n$	Methylene blue	2.21	20 mg	60	UV light	80.10	[70]
Dy-MOF + H_2O_2	Methylene blue	3.11	5 mg	25	Visible light	93	[58]
$\{[hmt][Cu_4I_5]^-[H_2O]_5[NH_4]^+\}_n$	Methylene blue	1.55	-	40	Visible light	70	[71]
$Zn_4O(BDC)_3$ MOF	Methylene Blue	3.2	-	60	UV light		[72]

PCN-250(Fe_2Mn)	Methylene blue	-	20 mg	290	Visible light	100	[54]
Sm-TCPP	Methylene blue	2.31	100 mg	100	50 W xenon lamp	73.80	[73]
$[Na_2Zn_3(btc)_2(\mu\text{-}HCOO)_2(\mu\text{-}H_2O)_8]_n$	Methylene blue	3.27	20 mg	80	Sunlight	93.69	[74]
ZIF-8@TA/CaAlg@TA	Methylene blue	-	3%	40	UV light	95.50	[75]
MIL-100(Fe)@PAN	Methyl orange	2.17	0.0616 ± 0.0147 g	60	Visible light	99	[52]
SOS-SH@ZIF-8	Methyl orange	-	120 mg/L	240	UV light	85.70	[76]
UiO-66/Palygorskite/TiO_2	Methyl orange	3.18	20 mg	90	UV light	78	[77]
$[Zn_2(odpt)(bpy)(H_2O)](bpy)_{0.5}]$	Methyl orange	3.60	50 mg	40	UV light	91.7	[53]
$[Cd(NDC)(biim\text{-}4)]\cdot 0.5H_2O$	Methyl orange	3.46	20 mg	180	UV light	92	[78]
UiO-66-NH_2@CNT	Methyl orange, rhodamine B	2.77	30 mg/L	30	LED light	100.93	[79]
NH_2-UiO-66/BiOBr/PVDF	Methylene blue, methyl orange, rhodamine	-	-	180	Visible light	99.2	[80]
BiOI/$ZnFe_2O_4$/MIL-88B(Fe)	Acid blue 92	2.1	10 mg	120	LED light	80	[55]
NH_2-MIL-101(Fe)	Turquoise blue	-	125 mg/L	1140	Visible light	86	[81]
CdS/Ce-MOF	Crystal violet	2.91	50 mg	40	Sunlight	90	[82]
$[Mn_2(L)(1,10\text{-}phen)(H_2O)]\cdot H_2O$	Methyl violet	-	50 mg	100	UV light	72.5	[83]
$[Dy_2(L^a)_2(ox)(H_2O)_4]$	Methyl violet	-	40 mg	40	UV light	74.3	[84]
$[Pb_4Cu_2I_2(pdc)_4(DMF)_6]_n$	Congo red	2.68	20 mg	25	UV light	>90	[85]
ZIF-8/HKUST-1	Congo red	3.73	10 mg	50	UV-LED	91.8	[86]
JUC-138	Azure B	3.34	-	240	UV light	90	[87]
AlOOH-ZrO_2-PCN	Orange II	3	20 mg	60	UV light	58	[88]
Ag_2O/ZnO/CuO	Acid Blue 92	3.30	-	45	Mercury-UV light	-	[89]
CuO-ZnO/ZIF-8	Acid Orange 7	1.96	0.1 g	100	Visible light	98.1	[90]
Dyes@Cu-MOF (BY24@1, BR14@1 and MB@1)	Reactive Blue 21	2.19, 2.10 and 1.76	35.81 mg/L	660	Visible light	89.0, 91.5 and 97.3	[91]

6. Photocatalytic Degradation of Other Pollutants

MOFs can be employed in the photodegradation process of many advanced pollutants, oxidation reactions, and dye photocatalysis. Table 3 below provides a visual representation of this information. As mentioned in Table 2, another type of pollutant that also exists in wastewater is phenolic compounds like p-nitrophenol. The previous research has conducted the synthesis of MOFs with two different metals, i.e., Zn and Cd, into MOFs $[Zn_2(L)(H_2O)(bib)]$ and $[Cd_2(L)(bib)]$, (5,5-(1,4-phenylenebis(methyleneoxy)diisophthalic acid (H_2L); 1,1'-(1,4-butanediyl)bis(imidazole) (bbi), and then tested these materials to degrade p-nitrophenol. The result of the studies showed that the $[Zn_2(L)(H_2O)(bib)]$ performs better photocatalytic activity than $[Cd_2(L)(bib)]$, achieving 90.01% of degradation of p-nitrophenol in 50 minutes[92)]

In MOFs, NH_2-UiO-66 is already known as a material for photocatalytic degradation because of its high absorption capacity. However, the low electron transport of this material must be solved by incorporating it with other high-conductivity materials like SAO ($SrAl_2O_4$: Eu^{2+}, Dy^{3+}). SAO has high thermal stability and has the properties to save energy after illumination. The solvothermal method has already been used to synthesize SAO/NH_2-UiO-66. The SAO/NH_2-UiO-66 was then employed to photodegrade pesticide waste imidacloprid under visible light, and it showed excellent performance.[93)]

Qin et al.[94)] have synthesized, characterized, and applied CdS/Zr-MOF. The synthesis of CdS/Zr-MOF necessitates the completion of multiple processes, one of which involves the synthesis of Zr-MOF. The G/Zr-MOF was synthesised using in situ G loading, followed by mild pyrolysis at 240 ºC to obtain the CdS/Zr-MOF. HR TEM images and EDX mapping characterization have confirmed the successful synthesized CdS/Zr-MOF. The resulting material was tested to photodegrade synthetic plastic Polyvinyl chloride (PVC). Unlike the general mechanism reactions of photocatalysis CO_2 and H_2O as products in PVC degradation, this research aims to degrade or convert the PVC into a smaller compound, i.e., acetic acid. CdS/Zr-MOF performs high photocatalytic activity, as shown by the percentage of PVC conversion reaching 76.5%. This material, CdS/Zr-MOF, is promising for degrading waste like PVC and yielding another valuable chemical.

Table 3. Photocatalysis of pollutants other than dyes using MOFs

Materials	Pollutants	Reference
Hf-NU-1000	Methyl phenyl sulfide	95)
Ru@dpdhpzBASF-A520	Hydrogen evolution reaction	96)
α-Fe_2O_3@MIL-101(Cr)@TiO_2	Paraquat	97)
$[Zn_2(L)(H_2O)(bbi)]$	p-nitrophenol	92)
$Ni_3(BTC)_2{\cdot}12H_2O$	4-nitrophenol (4-NP)	98)
SAO/NH_2-UiO-66	Imidacloprid	93)
SYD-1-CuNi	CO_2 reduction reaction and hydrogen evolution reaction	99)
Fe_3O_4/MIL-125	Tetracycline hydrochloride	100)
CdS/Zr-MOF	Polyvinyl chloride (PVC)	94)
UiO-66-NH_2(Zr/Ti)	Cr(IV) & Cr(III)	101)
MOF@COF	U(VI)	102)
MIL-53(Al)@ZnO	Naproxen, ibuprofen and methyl orange	103)
Zr-MOF/GO	Carbamazepine	104)
CoCeOx/g-C_3N_4	Carbamazepine	105)
MIL-53(Fe)	Phenol, metoprolol	106)
Zn-MOF-74	Glyphosate	107)
g-C_3N_4/UiO-66-NH_2	Acetaminophen	108)
TiO_2 /HKUST-1/CM	Ammonia	109)

6. Techniques for Characterizing the Degradation Pathways of MOFs During Pollutant Breakdown

To effectively utilize MOFs in pollution control, it is crucial to understand how these materials break down pollutants. This analysis requires a combination of advanced characterization techniques that reveal the degradation pathways and mechanisms. Liquid chromatography−mass spectrometry (LC-MS) is vital for understanding pollutant degradation mechanisms. Ray et al. used LC-MS to trace the norfloxacin (NFX) photodegradation pathway and identify reaction intermediates, revealing processes like ring opening, dihydroxylation, defluorination, and piperazinyl group cleavage, which reduce the pollutant's toxicity. They also highlighted the importance of ultraviolet-visible diffuse reflectance spectroscopy (UV-vis DRS) for evaluating band gap energy and light absorption in photocatalysis. Co-Zn-MOF-derived Co/C/N-ZnO nanoflakes with Ni_xP_y showed enhanced visible range absorption and improved photocatalytic performance[110]. In other work, Ray et al. explored the photodegradation mechanism of N_2 and H_2 in ZnO-Ni_xP_y composites under UV-vis light[111]. They also found that effective charge transfer at the semiconductor/electrolyte interface was verified through Electrochemical Impedance Spectroscopy (EIS), alongside observed charge migration and separation behavior within the ZnO-Ni_xP_y composite [112,113].

Behera et al. utilized UV-vis DRS and MS analysis to elucidate the photocatalytic mechanism of the CNZ/BCN-Ni_xP_y-2 nanocomposite. UV-vis DRS and MS analysis revealed CB and VB positions of C/N−ZnO (CNZ) as −0.69 and 2.42 V versus standard hydrogen electrode (SHE) and for /B-doped g-C_3N_4 (BCN) as −0.91 and 1.61 V versus SHE. Following a double charge transfer mechanism, photoinduced electrons move from BCN's higher CB to CNZ's lower CB under light irradiation, with holes migrating oppositely. X-ray photoelectron spectroscopy (XPS) analysis supports a Z-scheme charge transfer mechanism in H_2O_2 degradation, further validated by radical trapping tests[114].

7. Influences on the Photocatalytic Efficiency of Metal-Organic Frameworks

7.1. pH

pH level impacts the photocatalytic reaction process. This impact is due to its interference with the formation of active oxidants, the deionization of pollutants, and the alteration of the surface charge of the photocatalyst. Adding HCl to the GO(10)-ZIF-8/HKUST-1 surface caused a change in pH from 11 to 5, resulting in a positive charge on the surface. This effect of pH increased the degradation of congo red (anionic dye)[86]. The impact of pH on the degradation of carbamazepine on UiO-66/GO-05 was investigated within the pH range of 4-6. It was shown that carbamazepine degradation increased as the pH approached neutrality[104].

Furthermore, methyl orange degradation's pH was optimized using UiO-66/TiO_2 at a pH of 5. It was shown that the degradation of methyl orange increased at this pH level[77]. Adding TC-HCl to H-MIL-53 resulted in an accelerated degradation rate, which had the most significant impact at a pH value of 3[115]. According to prior research, the optimal pH range for the degradation of phenol and metoprolol in MIL-100 (Fe) is pH 4[106]. The pH impacts the glyphosate degradation process in Zn-MOF-74, where the negatively charged surface of the catalyst increases the degradation rate at pH 7.1[107]. The positive charge of Ag_2O/ZnO/CuO is adversely affected by a pH of 6.5, resulting in degradation[89]. The impact of pH on ACE in the presence of g-C_3N_4/UiO-66-NH_2 enhances the photocatalytic degradation process, with the most favorable pH value being 4.15[108]. The photocatalytic activity of CuO-ZnO/ZIF-8 in degrading AO7 is enhanced at pH 7[116].

The optimum pH for photodegradation can vary depending on the specific MOFs and the degraded target pollutant. However, many MOFs are generally stable across a broad range of pH values, typically between 3 and 9. It is important to note that while pH can influence the stability and activity of MOFs, other factors, such as the composition of the MOFs, the nature of the pollutant, and the light source used for photodegradation, also play crucial roles. Therefore, the optimal pH for photodegradation by a particular MOF would likely need to be tested experimentally under various pH conditions.

7.2. Concentration of Catalyst

The amount of catalyst is a crucial determinant of the rate at which the photocatalytic process occurs. Enhancing the amount of catalyst can improve the number of reaction sites, accelerating the photocatalytic reaction rate. Nevertheless, it is essential to note that excessive catalyst utilization does not consistently yield favorable catalytic efficiency. An excessive catalyst concentration might lead to light scattering, reduced light penetration, and catalyst aggregation[117].

7.3. Conditions of Light Irradiation

MOF materials can potentially undergo photochemical degradation when exposed to different lighting[118]. The impact of light conditions relies upon the wavelength and intensity of the light, wherein distinct wavelengths correspond to varying band gaps in the material[118]. Some studies mentioned above extensively use ultraviolet and visible light. However, in some studies, the composite catalyst exhibits enhanced degradation and superior performance within the visible light range. For instance, a study demonstrates that the Zn-MOF-74 composite has an absorption band at around 594 nm in visible light, resulting in a 75% degradation rate. This degradation is associated with a band gap of 2.09 eV[107]. Some papers

utilize UV light with absorption wavelengths below 387.7 nm on titania catalysts to induce a shift in the VB electrons with semiconductor surfaces[72].

7.4. The Structures of Materials

The photodegradation capabilities of MOFs are significantly impacted by their structural properties. First, analyzing and investigating the structure, morphology, elemental composition, electrochemical properties, and band structures requires a broad range of characterization techniques[119]. Multiple elements contribute to this phenomenon, such as crystal structure[120], the porosity of the MOFs, which dictates its capacity to sustain a porous structure without collapsing, the accessibility of its pores, its surface area[121], volume, connectivity, and particle size. Increasing the pores' size can improve the ability of the active sites to be reached, facilitating a more effective interaction between the MOFs and the desired molecules. As a result, the effectiveness of photodegradation is enhanced. Moreover, a larger pore size can improve the diffusion of the desired molecules into the MOF structure, resulting in interaction with the photocatalytic sites. Conversely, a smaller pore size could restrict the access of the target molecules to the active sites, which may decrease the effectiveness of photodegradation[122].

The photocatalytic activity of MOFs is also influenced by the characteristics of the ligand and the integration of different functional elements[122,123]. The ligand is an organic linker in the MOFs, and the substituents can change its energy band. Substituents with varied electron donating and withdrawing capacities can change the band energy of MOFs, influencing their light absorption and photocatalytic activity[124]. Late transition metal cations, N-containing ligands, and co-ligands are commonly used due to their strong coordinating ability with metal ions(110). As shown in Table 2, Zn MOFs with the BPEA ligand (NNU-36) exhibit outstanding performance, achieving up to 96.20% degradation in 60 minutes as opposed to only 85% for the Zn MOF with the BTC ligand in 90 minutes[61,63]. It indicates that the BPEA ligand is more effective in enhancing the degradation ability of Zn MOFs.

Moreover, metal ions and their arrangement inside the MOFs can influence their capacity for photodegradation [126]. For instance, Brahmi et al. have already investigated the impact of various metal ions on the degradation rate of acid black dyes. The MIL-53 (Cr)/polymer composite exhibited a degradation efficiency of 96% for acid black within 30 min, whereas the HKUST-1 (Cu)/polymer composite required 45 minutes to achieve a similar level of degradation[127]. Analysis of Table 2 reveals superior performance by the MOFs containing Cu metal ions in rhodamine B degradation compared to Zn. $Cu_3(BTC)_2$ + H_2O_2 achieves 99% degradation within 60 minutes, significantly surpassing the 85% achieved by Zn-BTC + H_2O_2 in 90 minutes[51,63]. This ability suggests a higher catalytic activity for Cu metal ions in degradation. Furthermore, the type of ligand also influences the degradation efficiency of MOFs.

Although there is no direct correlation between the predicted band gap values and the photocatalytic capacity of MOFs, it is possible to adjust their structural and electronic characteristics to improve their efficiency as photodegradation catalysts[128]. This method, such as doping, can avoid electron-hole pair recombination[129]. Hence, the design and engineering of the structure of MOFs are vital in determining their photodegradation ability[34,130].

7.5. The Stability and Reusability of Materials

Ensuring the durability and recyclability of materials are crucial factors in their utilization. It is essential to consider the amount of metal ions released from the metal-containing material known as MOFs throughout usage, as it indicates the material's stability. The stability of the solid was evaluated by examining the structure after the final cycle. It was found that the well-defined g-C_3N_4/UiO-66-NH_2 did not exhibit a decrease in intensity[108].

Numerous investigations have been carried out to comprehend the modifications in material structure that occur upon reuse. One of the experiments involved performing five consecutive reuse tests to evaluate the effectiveness of g-C_3N_4/UiO-66-NH_2 in removing acetaminophen (ACE). The results showed that ACE was eliminated after 180 minutes[108]. Lun Pan et al. reported that MOF-derived C-doped ZnO exhibits reusability, maintaining its activity after five degradation cycles[131]. Similarly, Chen et al. demonstrated the reusability of ZIF-8@TA/CaAlg@TA for methylene blue degradation, showing effectiveness for up to 10 cycles[75].

8. Challenges and Limitations of MOFs as a Photocatalyst

MOFs have shown considerable promise as photocatalysts due to their tunable structures, large surface areas, and potential for integrating various functional groups. However, several challenges and limitations hinder their practical application in this field. One significant challenge is the stability of MOFs under photocatalytic conditions. Many MOFs are prone to degradation when exposed to light, moisture, and reactive intermediates generated during photocatalysis. Also, utilizing MOFs in water purification technologies requires water-stable MOFs. These water-stable MOFs are characterized by their ability to maintain structural integrity when exposed to water molecules[132]. This instability can lead to a loss of catalytic activity over time, making long-term applications difficult. Moreover, synthesizing highly stable MOFs that can withstand harsh photocatalytic conditions without compromising their structural integrity remains a complex and resource-intensive task.

Another drawback is the efficiency of light absorption and charge separation in MOFs. Even though MOFs can be designed to include light-absorbing elements, their inherent photophysical properties often lead to poor absorption of visible light and inefficient charge separation. This inefficiency hinders the production of photo-induced charge carriers needed for photocatalytic reactions. Additionally, the recombination of electron-hole pairs within the MOF structure can significantly decrease the quantum efficiency of the photocatalytic process. Improving the light-harvesting capabilities and charge separation within MOFs necessitates innovative design strategies and adding extra components, such as co-catalysts or photosensitizers, which increase complexity and cost. Besides, MOFs' effectivity for photodegradation depends on pH and types of oxidants [133].

Lastly, MOFs' scalability and economic feasibility as photocatalysts pose considerable challenges[134]. The synthesis of MOFs often involves expensive starting materials, solvents, and conditions that could be more easily scalable. Furthermore, the production processes must be meticulously regulated to attain the targeted structural and functional characteristics. For MOFs to be feasible for extensive industrial applications, it is essential to develop synthesis methods that are both cost-efficient and scalable. Additionally, integrating MOFs into practical photocatalytic systems, such as reactors or devices, necessitates overcoming challenges associated with material handling, dispersion, and compatibility with current technologies. Overcoming these economic and practical constraints is vital to adopting MOFs as effective photocatalysts.

9. Conclusion and Outlook

MOFs exhibit significant potential as photocatalysts for dye degradation, presenting a promising solution to the environmental pollution caused by synthetic dyes. Their highly porous structures, tunable chemical properties, and large surface areas facilitate efficient light absorption and the generation of reactive species necessary for dye degradation. Recent studies have demonstrated that MOFs and their composites can degrade various dyes under visible light, highlighting their versatility and effectiveness. However, challenges such as stability under operational conditions, potential toxicity, and the cost of large-scale production remain areas needing further research and development.

The future of MOFs as photocatalysts for dye degradation is promising, with ongoing advancements in materials science and engineering likely to address current limitations. Innovations in synthesis techniques may enhance the stability and reusability of MOFs, making them more practical for industrial applications. Additionally, combining MOFs with other materials, such as semiconductors or metal nanoparticles, could improve their photocatalytic efficiency and broaden their applicability. As our understanding of the photocatalytic mechanisms of MOFs deepens, it will be possible to design more efficient and targeted MOFs for specific dye pollutants, further optimizing their performance.

Future research on MOFs as photocatalysts should focus on several key areas to maximize their potential. First, developing more robust and cost-effective synthesis methods is essential for scaling production. Second, comprehensive studies on MOFs' long-term stability and recyclability in various environmental conditions are necessary to ensure their practical application. Third, exploring MOFs' ecological and health impacts will be crucial to address any potential risks associated with their use. Finally, interdisciplinary approaches combining computational modeling, advanced characterization techniques, and experimental validation will accelerate the discovery of new MOFs with enhanced photocatalytic properties for efficient and sustainable dye degradation.

Nomenclature

Ref.	References
Ev	Electron volt
LED	Light-emitting Diode
HR TEM	High Resolution Transmission Electron Microscopy
EDX	Energy-dispersive X-ray

References

1) C.M. Hussain, M.S. Paulraj, and S. Nuzhat, "Source reduction and waste minimization in textile industries," *Source Reduction and Waste Minimization*, 159–168 (2022). doi:10.1016/B978-0-12-824320-6.00010-1.
2) F. Amalina, A.S.A. Razak, S. Krishnan, A.W. Zularisam, and M. Nasrullah, "Dyes removal from textile wastewater by agricultural waste as an absorbent – a review," *Cleaner Waste Systems*, **3** (2022). doi:10.1016/j.clwas.2022.100051.
3) E.J. Cho, Y.G. Lee, Y. Song, H.Y. Kim, D.T. Nguyen, and H.J. Bae, "Converting textile waste into value-added chemicals: an integrated bio-refinery process," *Environmental Science and Ecotechnology*, **15** (2023). doi:10.1016/j.ese.2023.100238.
4) A. Bhava, U.S. Shenoy, and D.K. Bhat, "Silver doped barium titanate nanoparticles for enhanced visible light photocatalytic degradation of dyes," *Environmental Pollution*, **344** 123430 (2024). doi:10.1016/J.ENVPOL.2024.123430.
5) D. Dhaneswara, N. Zulfikar, J.F. Fatriansyah, M.S. Mastuli, and I. Suhariadi, "Adsorption capacity of mesoporous sba-15 particles synthesized from corncobs and rice husk at different ctab/p123 ratios and their application for dyes adsorbent," *Evergreen*, **10** (*2*) 924–930 (2023). doi:10.5109/6792887.
6) R. Al-Tohamy, S.S. Ali, F. Li, K.M. Okasha, Y.A.G.

Mahmoud, T. Elsamahy, H. Jiao, Y. Fu, and J. Sun, "A critical review on the treatment of dye-containing wastewater: ecotoxicological and health concerns of textile dyes and possible remediation approaches for environmental safety," *Ecotoxicol Environ Saf*, **231** (2022). doi:10.1016/j.ecoenv.2021.113160.

7) J. Yu, L. Bai, Z. Feng, L. Chen, S. Xu, and Y. Wang, "Waste treats waste: facile fabrication of porous adsorbents from recycled pet and sodium alginate for efficient dye removal," *Chemosphere*, 141738 (2024). doi:10.1016/J.CHEMOSPHERE.2024.141738.
8) R. Muhammad, and S. Adityosulindro, "Biosorption of brilliant green dye from synthetic wastewater by modified wild algae biomass," *Evergreen*, **9** (*1*) 133–140 (2022). doi:10.5109/4774228.
9) M. Kaur, N. Mittal, A. Charak, A.P. Toor, and V. Singh, "Rice husk derived activated carbon for the adsorption of scarlet rr an anionic disperse dye," *EVERGREEN Joint Journal of Novel Carbon Resource Sciences & Green Asia Strategy*, **10**(1) 438–443 (2023). doi:10.5109/6782146
10) E. Ali, I. Amjad, and A. Rehman, "Evaluation of azo dyes degradation potential of fungal strains and their role in wastewater treatment," *Saudi J Biol Sci*, **30** (*8*) (2023). doi:10.1016/j.sjbs.2023.103734.
11) P.O. Oladoye, T.O. Ajiboye, E.O. Omotola, and O.J. Oyewola, "Methylene blue dye: toxicity and potential elimination technology from wastewater," *Results in Engineering*, **16** (2022). doi:10.1016/j.rineng.2022.100678.
12) Y. Iriani, R. Afriani, K. Sandi, and F. Nurosyid, "Co-precipitation Synthesis and Photocatalytic Activity of Mn-doped SrTiO 3 for the Degradation of Methylene Blue Wastewater," 2022.
13) R. Singh Sinsinwar, and M. Verma, "Analysis of ph value of water for treatment plant of kekri and surajpura (rajasthan) india," *Evergreen Joint Journal of Novel Carbon Resource Sciences & Green Asia Strategy*, **10**(1) 324–328 (2023). doi:10.5109/6781087
14) A.S. Rini, Y. Rati, R. Fadillah, R. Farma, L. Umar, and Y. Soerbakti, "Improved photocatalytic activity of zno film prepared via green synthesis method using red watermelon rind extract," *EVERGREEN Joint Journal of Novel Carbon Resource Sciences & Green Asia Strategy*, **09**(4) 1046–1055 (2022). doi:10.5109/6625718
15) Z. Arifin, S. Hadi, Suyitno, B. Sutanto, and D. Widhiyanuriyawan, "Investigation of curcumin and chlorophyll as mixed natural dyes to improve the performance of dye-sensitized solar cells," *Evergreen*, **9** (*1*) 17–22 (2022). doi:10.5109/4774212.
16) P. Kumari, and A. Kumar, "ADVANCED oxidation process: a remediation technique for organic and non-biodegradable pollutant," *Results in Surfaces and Interfaces*, **11** (2023). doi:10.1016/j.rsurfi.2023.100122.
17) Mu'to Naimah, F. Dellarosa Nanda Pratama, and M. Ibadurrohman, "Photocatalytic hydrogen production using fe-graphene/tio2 photocatalysts in the presence of polyalcohols as sacrificial agents," *EvergreenJoint Journal of Novel Carbon Resource Sciences & Green Asia Strategy*, **09** (4) 1244–1251 (2022). doi:10.5109/6625736
18) D.G. Domínguez-Talamantes, D. Vargas-Hernández, J.T. Hernández-Oloño, E. Rodríguez-Castellón, M. Arellano-Cortaza, S.J. Castillo, and J.C. Tánori-Córdova, "Enhanced photocatalytic activity of feso4 in a zno photocatalyst with h2o2 for dye degradation," *Optik (Stuttg)*, 171753 (2024). doi:10.1016/J.IJLEO.2024.171753.
19) A. V. Mohod, M. Momotko, N.S. Shah, M. Marchel, M. Imran, L. Kong, and G. Boczkaj, "Degradation of rhodamine dyes by advanced oxidation processes (aops) – focus on cavitation and photocatalysis - a critical review," *Water Resour Ind*, **30** (2023). doi:10.1016/j.wri.2023.100220.
20) Y. Kondo, Y. Kuwahara, K. Mori, and H. Yamashita, "Design of metal-organic framework catalysts for photocatalytic hydrogen peroxide production," *Chem*, **8** (*11*) 2924–2938 (2022). doi:10.1016/j.chempr.2022.10.007.
21) O.K. Akeremale, O.T. Ore, A.A. Bayode, H. Badamasi, J. Adedeji Olusola, and S.S. Durodola, "Synthesis, characterization, and activation of metal organic frameworks (mofs) for the removal of emerging organic contaminants through the adsorption-oriented process: a review," *Results Chem*, **5** (2023). doi:10.1016/j.rechem.2023.100866.
22) W. Shi, W. Li, W. Nguyen, W. Chen, J. Wang, and M. Chen, "Advances of metal organic frameworks in analytical applications," *Mater Today Adv*, **15** (2022). doi:10.1016/j.mtadv.2022.100273.
23) S.F. Hammad, I.A. Abdallah, A. Bedair, R.M. Abdelhameed, M. Locatelli, and F.R. Mansour, "Metal organic framework-derived carbon nanomaterials and mof hybrids for chemical sensing," *TrAC Trends in Analytical Chemistry*, **170** 117425 (2024). doi:10.1016/j.trac.2023.117425.
24) H.W.B. Teo, and A. Chakraborty, "Methane adsorption characteristics of hkust-1 and mil-101(cr) using gcmc (grand canonical monte carlo) simulation," *Evergreen*, **2** (*2*) 44–49 (2015). doi:10.5109/1544079.
25) F. Yulia, S. Marsya, Y. Bobby, Nasruddin, and A. Zulys, "Design and preparation of succinic acid-based metal-organic frameworks for co2 adsorption technology," *Evergreen*, **7** (*4*) 549–554 (2020). doi:10.5109/4150475.
26) P. Li, J. Li, X. Feng, J. Li, Y. Hao, J. Zhang, H. Wang, A. Yin, J. Zhou, X. Ma, and B. Wang, "Metal-organic frameworks with photocatalytic bactericidal activity for integrated air cleaning," *Nat Commun*, **10** (*1*) 2177 (2019). doi:10.1038/s41467-019-10218-9.
27) N.J. Castellanos, Z. Martinez Rojas, H.A. Camargo, S. Biswas, and G. Granados-Oliveros, "Congo red decomposition by photocatalytic formation of hydroxyl radicals (·oh) using titanium metal–organic frameworks," *Transition Metal Chemistry*, **44** (*1*)

77–87 (2019). doi:10.1007/s11243-018-0271-z.
28) Y.L. Wang, S. Zhang, Y.F. Zhao, J. Bedia, J.J. Rodriguez, and C. Belver, "UiO-66-based metal organic frameworks for the photodegradation of acetaminophen under simulated solar irradiation," *J Environ Chem Eng*, **9** (*5*) 106087 (2021). doi:10.1016/J.JECE.2021.106087.
29) Z. Wu, Y. Li, C. Zhang, X. Huang, B. Peng, and G. Wang, "Recent advances in metal-organic-framework-based catalysts for thermocatalytic selective oxidation of organic substances," *Chem Catalysis*, **2** (*5*) 1009–1045 (2022). doi:10.1016/j.checat.2022.02.010.
30) X. Liu, Y. Shan, S. Zhang, Q. Kong, and H. Pang, "Application of metal organic framework in wastewater treatment," *Green Energy and Environment*, **8** (*3*) 698–721 (2023). doi:10.1016/j.gee.2022.03.005.
31) S.Z.M. Murtaza, H.T. Alqassem, R. Sabouni, and M. Ghommem, "Degradation of micropollutants by metal organic framework composite-based catalysts: a review," *Environ Technol Innov*, **29** (2023). doi:10.1016/j.eti.2022.102998.
32) G. Zhou, Y. Wang, and Z. Huang, "Structure and function tailored metal-organic frameworks for heterogeneous catalysis," *Chem Catalysis*, **2** (*12*) 3304–3319 (2022). doi:10.1016/j.checat.2022.10.023.
33) X. Chen, L. Qiao, R. Zhao, J. Wu, J. Gao, L. Li, J. Chen, W. Wang, M.G. Galloni, F.M. Scesa, Z. Chen, and E. Falletta, "Recent advances in photocatalysis on cement-based materials," *J Environ Chem Eng*, **11** (*2*) (2023). doi:10.1016/j.jece.2023.109416.
34) S. Subudhi, S.P. Tripathy, and K. Parida, "Metal oxide integrated metal organic frameworks (mo@mof): rational design, fabrication strategy, characterization and emerging photocatalytic applications," *Inorg Chem Front*, **8** (*6*) 1619–1636 (2021). doi:10.1039/D0QI01117G.
35) S.P. Tripathy, S. Subudhi, A. Ray, P. Behera, A. Bhaumik, and K. Parida, "Mixed-valence bimetallic ce/zr mof-based nanoarchitecture: a visible-light-active photocatalyst for ciprofloxacin degradation and hydrogen evolution," *Langmuir*, **38** (*5*) 1766–1780 (2022). doi:10.1021/acs.langmuir.1c02873.
36) S.P. Tripathy, S. Subudhi, A. Ray, P. Behera, G. Swain, M. Chakraborty, and K. Parida, "MgIn2S4/uio-66-nh2 mof-based heterostructure: visible-light-responsive z-scheme-mediated synergistically enhanced photocatalytic performance toward hydrogen and oxygen evolution," *Langmuir*, **39** (*21*) 7294–7306 (2023). doi:10.1021/acs.langmuir.3c00151.
37) S.P. Tripathy, S. Subudhi, A. Ray, P. Behera, and K. Parida, "Metal organic framework-based janus nanomaterials: rational design, strategic fabrication and emerging applications," *Dalton Transactions*, **51** (*14*) 5352–5366 (2022). doi:10.1039/D1DT04380C.
38) R. Ramadhan Ikreedeegh, M. Arif Hossen, A. Sherryna, and M. Tahir, "Recent advances on the synthesis and photocatalytic applications of mof-derived carbon materials: a review," *Coord Chem Rev*, **510** (*April*) 215834 (2024). doi:10.1016/j.ccr.2024.215834.
39) J. Zhang, H. Wu, L. Shi, Z. Wu, S. Zhang, S. Wang, and H. Sun, "Photocatalysis coupling with membrane technology for sustainable and continuous purification of wastewater," *Sep Purif Technol*, **329** (2024). doi:10.1016/j.seppur.2023.125225.
40) X. Li, Y. Chen, Y. Tao, L. Shen, Z. Xu, Z. Bian, and H. Li, "Challenges of photocatalysis and their coping strategies," *Chem Catalysis*, **2** (*6*) 1315–1345 (2022). doi:10.1016/j.checat.2022.04.007.
41) N.I.I. Zamri, S.L.N. Zulmajdi, E. Kusrini, K. Ayuningtyas, H.M. Yasin, and A. Usman, "Rhodamine b photocatalytic degradation using CuO particles under uv light irradiation for applications in industrial and medical fields," *Evergreen*, **7** (*2*) 280–284 (2020). doi:10.5109/4055233.
42) N.M. Mahmoodi, J. Abdi, M. Oveisi, M. Alinia Asli, and M. Vossoughi, "Metal-organic framework (mil-100 (fe)): synthesis, detailed photocatalytic dye degradation ability in colored textile wastewater and recycling," *Mater Res Bull*, **100** (*December 2017*) 357–366 (2018). doi:10.1016/j.materresbull.2017.12.033.
43) S. Naghdi, M.M. Shahrestani, M. Zendehbad, H. Djahaniani, H. Kazemian, and D. Eder, "Recent advances in application of metal-organic frameworks (mofs) as adsorbent and catalyst in removal of persistent organic pollutants (pops)," *J Hazard Mater*, **442** (*September 2022*) 130127 (2023). doi:10.1016/j.jhazmat.2022.130127.
44) H. Widiyandari, Y. Ayash, M. Shalahuddin, A. Ja'farawy, A. Subagio, and W.B. Widayatno, "Synthesis of WO 3 /Pt Nanoparticle by Microwave-assisted Sol-gel Method for Enhanced Photocatalytic Property in Visible Light," 2023.
45) A. Azani, D.S.C. Halin, M.M. Al Bakri Abdullah, K.A. Razak, M.F.S.A. Razak, M.M. din Ramli, M.A.A.M. Salleh, and V. Chobpattana, "The effect of go/tio2 thin film during photodegradation of methylene blue dye," *Evergreen*, **8** (*3*) 556–564 (2021). doi:10.5109/4491643.
46) M.S. Samuel, K.V. Savunthari, and S. Ethiraj, "Synthesis of a copper (ii) metal–organic framework for photocatalytic degradation of rhodamine b dye in water," *Environmental Science and Pollution Research*, **28** (*30*) 40835–40843 (2021). doi:10.1007/s11356-021-13571-9.
47) D.E. Lee, M.K. Kim, M. Danish, and W.K. Jo, "State-of-the-art review on photocatalysis for efficient wastewater treatment: attractive approach in photocatalyst design and parameters affecting the photocatalytic degradation," *Catal Commun*, **183** (2023). doi:10.1016/j.catcom.2023.106764.
48) D. Pathak, A. Sharma, D.P. Sharma, and V. Kumar, "A review on electrospun nanofibers for photocatalysis: upcoming technology for energy and

environmental remediation applications," *Applied Surface Science Advances*, **18** (2023). doi:10.1016/j.apsadv.2023.100471.

49) T. Velempini, E. Prabakaran, and K. Pillay, "Recent developments in the use of metal oxides for photocatalytic degradation of pharmaceutical pollutants in water—a review," *Mater Today Chem*, **19** 100380 (2021). doi:10.1016/j.mtchem.2020.100380.
50) A. Sharma, M. Tahir, T. Ahamad, N. Kumar, S. Sharma, M. Kumari, M.A. Majeed Khan, S. Takhur, and P. Raizada, "Improved charge transfer and enhanced visible light photocatalytic activity of bi2o3@fe-mof for degradation of rhodamine b and triclopyr," *J King Saud Univ Sci*, **35** (*10*) 102922 (2023). doi:10.1016/J.JKSUS.2023.102922.
51) M.S. Samuel, K.V. Savunthari, and S. Ethiraj, "Synthesis of a copper (ii) metal–organic framework for photocatalytic degradation of rhodamine b dye in water," *Environmental Science and Pollution Research*, **28** (*30*) 40835–40843 (2021). doi:10.1007/s11356-021-13571-9.
52) H. Lee, H. Lee, S. Ahn, and J. Kim, "MIL-100(fe)-hybridized nanofibers for adsorption and visible light photocatalytic degradation of water pollutants: experimental and dft approach," *ACS Omega*, **7** (*24*) 21145–21155 (2022). doi:10.1021/acsomega.2c01953.
53) C.C. Wang, Y.Q. Zhang, T. Zhu, P. Wang, and S.J. Gao, "Photocatalytic degradation of methylene blue and methyl orange in a zn(ii)-based metal–organic framework," *Desalination Water Treat*, **57** (*38*) 17844–17851 (2016). doi:10.1080/19443994.2015.1088807.
54) A. Kirchon, P. Zhang, J. Li, E.A. Joseph, W. Chen, and H.C. Zhou, "Effect of isomorphic metal substitution on the fenton and photo-fenton degradation of methylene blue using fe-based metal-organic frameworks," *ACS Appl Mater Interfaces*, **12** (*8*) 9292–9299 (2020). doi:10.1021/acsami.9b21408.
55) S.G. Khasevani, and M.R. Gholami, "Synthesis of bioi/znfe2o4-metal-organic framework and g-c3n4-based nanocomposites for applications in photocatalysis," *Ind Eng Chem Res*, **58** (*23*) 9806–9818 (2019). doi:10.1021/acs.iecr.8b05871.
56) M. Hossein Zadeh, N. Keramati, and M. Mehdipour Ghazi, "The effect of solvents on photocatalytic activity of fe-btc metal organic framework obtained via sonochemical method," *Inorganic and Nano-Metal Chemistry*, **49** (*12*) 448–454 (2019). doi:10.1080/24701556.2019.1661455.
57) Q. Xia, X. Yu, H. Zhao, S. Wang, H. Wang, Z. Guo, and H. Xing, "Syntheses of novel lanthanide metal-organic frameworks for highly efficient visible-light-driven dye degradation," *Cryst Growth Des*, **17** (*8*) 4189–4195 (2017). doi:10.1021/acs.cgd.7b00504.
58) S. T.K, R. Pavithran, and S. Mohan M.R, "Crystal structure and photocatalytic activity of luminescent 3d-supramolecular metal organic framework of dysprosium," *Heliyon*, **9** (*11*) (2023). doi:10.1016/j.heliyon.2023.e21262.
59) K.T. Amakiri, A. Angelis-Dimakis, and A.R. Canon, "Recent advances, influencing factors, and future research prospects using photocatalytic process for produced water treatment," *Water Science and Technology*, **85** (*3*) 769–788 (2022). doi:10.2166/wst.2021.641.
60) A. Kumar, and G. Pandey, "A review on the factors affecting the photocatalytic degradation of hazardous materials," *Material Science & Engineering International Journal*, **1** (*3*) (2017). doi:10.15406/mseij.2017.01.00018.
61) H. Zhao, Q. Xia, H. Xing, D. Chen, and H. Wang, "Construction of pillared-layer mof as efficient visible-light photocatalysts for aqueous cr(vi) reduction and dye degradation," *ACS Sustain Chem Eng*, **5** (*5*) 4449–4456 (2017). doi:10.1021/acssuschemeng.7b00641.
62) H. Haroon, and K. Majid, "MnO2 nanosheets supported metal–organic framework mil-125(ti) towards efficient visible light photocatalysis: kinetic and mechanistic study," *Chem Phys Lett*, **745** (2020). doi:10.1016/j.cplett.2020.137283.
63) A. Sarkar, A. Adhikary, A. Mandal, T. Chakraborty, and D. Das, "Zn-btc mof as an adsorbent for iodine uptake and organic dye degradation," *Cryst Growth Des*, **20** (*12*) 7833–7839 (2020). doi:10.1021/acs.cgd.0c01015.
64) S.R. Zhu, M.K. Wu, W.N. Zhao, P.F. Liu, F.Y. Yi, G.C. Li, K. Tao, and L. Han, "In situ growth of metal-organic framework on biobr 2d material with excellent photocatalytic activity for dye degradation," *Cryst Growth Des*, **17** (*5*) 2309–2313 (2017). doi:10.1021/acs.cgd.6b01811.
65) R. Yu, Y. Shang, X. Zhang, J. Liu, F. Zhang, X. Du, H. Sun, and J. Zeng, "Self-templated synthesis of core-shell fe3o4@zno@zif-8 as an efficient visible-light-driven photocatalyst," *Catal Commun*, **174** 106583 (2023). doi:10.1016/J.CATCOM.2022.106583.
66) J. Du, J. Zhang, T. Yang, R. Liu, Z. Li, D. Wang, T. Zhou, Y. Liu, C. Liu, and G. Che, "The research on the construction and the photocatalytic performance of bioi/nh 2-mil-125(ti) composite," (2020). doi:10.3390/catal.
67) W. Lou, L. Wang, S. Dong, Z. cao, J. Sun, and Y. Zhang, "A facility synthesis of bismuth-iron bimetal mof composite silver vanadate applied to visible light photocatalysis," *Opt Mater (Amst)*, **126** (*March*) 112168 (2022). doi:10.1016/j.optmat.2022.112168.
68) M. Ishfaq, S.A. Khan, M.A. Nazir, S. Ali, M. Younas, M. Mansha, S.S.A. Shah, M. Arshad, and A. ur Rehman, "The in situ synthesis of sunlight-driven chitosan/mno2@mof-801 nanocomposites for photocatalytic reduction of rhodamine-b," *J Mol Struct*, **1301** (*November 2023*) 137384 (2024). doi:10.1016/j.molstruc.2023.137384.
69) Z. Huang, Q. Zhou, J. Wang, and Y. Yu, "Fermi-level-tuned mof-derived n-zno@nc for

photocatalysis: a key role of pyridine-n-zn bond," *J Mater Sci Technol*, **112** 68–76 (2022). doi:10.1016/j.jmst.2021.10.017.

70) F. Wang, F. Tian, Y. Deng, L. Yang, H. Zhang, D. Zhao, B. Li, X. Zhang, and L. Fan, "Cluster-based multifunctional copper(ii) organic framework as a photocatalyst in the degradation of organic dye and as an electrocatalyst for overall water splitting," *Cryst Growth Des*, **21** (*7*) 4242–4248 (2021). doi:10.1021/acs.cgd.1c00479.
71) X. Qiao, Y. Ge, Y. Li, Y. Niu, and B. Wu, "Preparation and analyses of the multifunctional properties of 2d and 3d mofs constructed from copper(i) halides and hexamethylenetetramine," *ACS Omega*, **4** (*7*) 12402–12409 (2019). doi:10.1021/acsomega.9b01356.
72) S.M. Ramteke, and S.R. Thakare, "SYNTHESIS OF Zn4O(BDC)3-(MOF-5) AND ITS APPLICATION AS PHOTOCATALYST," 2014. https://www.researchgate.net/publication/330703081.
73) F.C. Herrera, R.M. Caraballo, G.J.A.A. Soler Illia, G.E. Gomez, and M. Hamer, "Sunlight-driven photocatalysis for a set of 3d metal–porphyrin frameworks based on a planar tetracarboxylic ligand and lanthanide ions," *ACS Omega*, (2023). doi:10.1021/acsomega.3c06153.
74) A. Ali, M. Muslim, I. Neogi, M. Afzal, A. Alarifi, and M. Ahmad, "Construction of a 3d metal-organic framework and its composite for water remediation via selective adsorption and photocatalytic degradation of hazardous dye," *ACS Omega*, **7** (*28*) 24438–24451 (2022). doi:10.1021/acsomega.2c01869.
75) Y.X. Chen, Y.M. Yuan, H.Y. Yang, Q. Wang, Y. Ren, X.H. Guo, P. Zhang, M.J. Zhang, W. Wang, and L.Y. Chu, "Hierarchical porous tannic-acid-modified mofs/alginate particles with synergized adsorption-photocatalysis for water remediation," *Sep Purif Technol*, **330** (*PB*) 125435 (2024). doi:10.1016/j.seppur.2023.125435.
76) A. Ahmed, M. Forster, J. Jin, P. Myers, and H. Zhang, "Tuning morphology of nanostructured zif-8 on silica microspheres and applications in liquid chromatography and dye degradation," *ACS Appl Mater Interfaces*, **7** (*32*) 18054–18063 (2015). doi:10.1021/acsami.5b04979.
77) T. Ioannidou, M. Anagnostopoulou, D. Papoulis, K.C. Christoforidis, and I.A. Vasiliadou, "UiO-66/palygorskite/tio2 ternary composites as adsorbents and photocatalysts for methyl orange removal," *Applied Sciences (Switzerland)*, **12** (*16*) (2022). doi:10.3390/app12168223.
78) C. Zhang, D. Ma, X. Zhang, J. Ma, L. Liu, and X. Xu, "Preparation, structure and photocatalysis of metal-organic frameworks derived from aromatic carboxylate and imidazole-based ligands," *J Coord Chem*, **69** (*6*) 985–995 (2016). doi:10.1080/00958972.2016.1154145.
79) J. Abdi, F. Banisharif, and A. Khataee, "Amine-functionalized zr-mof/cnts nanocomposite as an efficient and reusable photocatalyst for removing organic contaminants," *J Mol Liq*, **334** 116129 (2021). doi:10.1016/j.molliq.2021.116129.
80) L. Peng, Y. Shu, L. Jiang, W. Liu, G. Zhao, and R. Zhang, "A new strategy of chemical photo grafting metal organic framework to construct nh2-uio-66/biobr/pvdf photocatalytic membrane for synergistic separation and self-cleaning dyes," *Molecules*, **28** (*22*) 7667 (2023). doi:10.3390/molecules28227667.
81) X. Li, Y. Wang, and Q. Guo, "Porous nh2-mil-101(fe) metal organic framework for effective photocatalytic degradation of azo dye in wastewater treatment," *Heliyon*, **8** (*7*) (2022). doi:10.1016/j.heliyon.2022.e09942.
82) J. Meng, M. He, F. Li, T. Li, Z. Huang, and W. Cao, "Combining ce-metal–organic framework with cds for efficient photocatalytic removals of heavy metal ion and organic pollutant under visible and solar lights," *Inorganica Chim Acta*, **557** (2023). doi:10.1016/j.ica.2023.121701.
83) L. Lu, J. Wang, S.L. Cai, B. Xie, B.H. Li, J.H. Man, Y.X. He, A. Singh, and A. Kumar, "Efficient photocatalytic degradation of methyl violet with two metall–organic frameworks," *J Coord Chem*, **70** (*19*) 3409–3421 (2017). doi:10.1080/00958972.2017.1390224.
84) F. Yuan, X.J. Wang, H.X. Ma, C.S. Zhou, C.F. Qiao, B.Y. Cao, H.C. Wang, A.K. Singh, A. Kumar, and M. Muddassir, "Synthesis, structure and photocatalysis of a new 3d dy(iii)-based metal-organic framework with carboxylate functionalized triazole derivative ligand," *J Mol Struct*, **1238** (2021). doi:10.1016/j.molstruc.2021.130388.
85) X.Y. Li, Y.L. Wang, Z. Xue, S. De Han, Z.Z. Xue, and J. Pan, "Heterometallic-organic framework from [cu2i2] and [pbo]nchains: photoluminescence, sensing, and photocatalytic performance," *Cryst Growth Des*, **21** (*9*) 5261–5267 (2021). doi:10.1021/acs.cgd.1c00588.
86) R. Ediati, L.L. Zulfa, I. Maulidah, D.O. Sulistiono, H. Fansuri, A. Rosyidah, F. Martak, D. Hartanto, M.A.B. Abdullah, W.P. Utomo, E.N. Kusumawati, and M. Shirai, "Addition of graphene oxide to zif-8/hkust-1 composite for enhanced adsorptive and photocatalytic removal of congo red in wastewater," *S Afr J Chem Eng*, **46** 132–142 (2023). doi:10.1016/j.sajce.2023.07.006.
87) N. Zhao, F. Sun, N. Zhang, and G. Zhu, "Novel pyrene-based anionic metal-organic framework for efficient organic dye elimination," *Cryst Growth Des*, **17** (*5*) 2453–2457 (2017). doi:10.1021/acs.cgd.6b01864.
88) I. Koltsov, J. Wojnarowicz, P. Nyga, J. Smalc-Koziorowska, S. Stelmakh, A. Babyszko, A.W. Morawski, and W. Lojkowski, "Novel photocatalytic nanocomposite made of polymeric carbon nitride and metal oxide nanoparticles," *Molecules*, **24** (*5*) (2019). doi:10.3390/molecules24050874.

89) H. Salari, and M. Sadeghinia, "MOF-templated synthesis of nano ag 2 o/zno/cuo heterostructure for photocatalysis," *J Photochem Photobiol A Chem*, **376** 279–287 (2019). doi:10.1016/j.jphotochem.2019.03.010.
90) B. Abdollahi, A. Najafidoust, E. Abbasi Asl, and M. Sillanpaa, "Fabrication of zif-8 metal organic framework (mofs)-based cuo-zno photocatalyst with enhanced solar-light-driven property for degradation of organic dyes," *Arabian Journal of Chemistry*, **14** (*12*) 103444 (2021). doi:10.1016/J.ARABJC.2021.103444.
91) Q. Li, Z. Fan, L. Zhang, Y. Li, C. Chen, R. Zhao, and W. Zhu, "Boosting and tuning the visible photocatalytic degradation performances towards reactive blue 21 via dyes@mof composites," *J Solid State Chem*, **269** 465–475 (2019). doi:10.1016/j.jssc.2018.10.025.
92) H.S. Bin, H. Hu, J. Wang, L. Lu, M. Muddassir, D. Srivastava, R. Chauhan, Y. Wu, X. Wang, and A. Kumar, "New 5,5-(1,4-phenylenebis(methyleneoxy)diisophthalic acid appended zn(ii) and cd(ii) mofs as potent photocatalysts for nitrophenols," *Molecules*, **28** (*20*) (2023). doi:10.3390/molecules28207180.
93) S.S. Li, L. Wen, S.W. He, Z. Xu, L. Ding, Y.H. Cheng, and M.L. Chen, "Enhanced photocatalytic degradation of imidacloprid by a simple z-type binary heterojunction composite of long afterglow with metal-organic framework," *Catal Commun*, **183** (2023). doi:10.1016/j.catcom.2023.106775.
94) J. Qin, Y. Dou, J. Zhou, D. Zhao, T. Orlander, H.R. Andersen, C. Hélix-Nielsen, and W. Zhang, "Encapsulation of carbon-nanodots into metal-organic frameworks for boosting photocatalytic upcycling of polyvinyl chloride plastic," *Appl Catal B*, **341** (2024). doi:10.1016/j.apcatb.2023.123355.
95) B. Zeng, W. Sheng, F. Huang, K. Zhang, K. Xiong, and X. Lang, "Cooperative photocatalysis of hafnium-based metal-organic framework and tempo for selective oxidation of sulfides," *Chemical Engineering Journal*, **474** (*145559*) 1–10 (2023). doi:10.1016/j.cej.2023.145559.
96) R. Rojas-Luna, J. Amaro-Gahete, D.G. Gil-Gavilán, M. Castillo-Rodríguez, C. Jiménez-Sanchidrián, J.R. Ruiz, D. Esquivel, and F.J. Romero-Salguero, "Visible-light-harvesting basolite-a520 metal organic framework for photocatalytic hydrogen evolution," *Microporous and Mesoporous Materials*, **355** (2023). doi:10.1016/j.micromeso.2023.112565.
97) A. Khodkar, S.M. Khezri, A. Pendashteh, S. Khoramnejadian, and L. Mamani, "Preparation and application of α-fe2o3@mil-101(cr)@tio2 based on metal–organic framework for photocatalytic degradation of paraquat," *Toxicol Ind Health*, **34** (*12*) 842–859 (2018). doi:10.1177/0748233718797247.
98) A. Arroussi, H. Gaffour, M. Mokhtari, and L. Boukli-Hacene, "Investigating metal-organic framework based on nickel (ii) and benzene 1,3,5-tri carboxylic acid (h3btc) as a new photocatalyst for degradation of 4-nitrophenol," *International Journal of Environmental Studies*, **77** (*1*) 137–151 (2020). doi:10.1080/00207233.2019.1584479.
99) W. Liang, M.Z.M. Noor, W. Lewis, A. Macmillan, X. Zhang, R. Tang, A. Kochubei, D. Wiley, B.S. Haynes, and J. Huang, "Design of an ocu-metal-organic framework for a photocatalysis reaction," *ChemPhotoChem*, **7** (*7*) (2023). doi:10.1002/cptc.202300031.
100) W. Liu, J. Zhou, D. Liu, S. Liu, X. Liu, and S. Xiao, "Enhancing electronic transfer by magnetic iron materials and metal-organic framework via heterogeneous fenton-like process and photocatalysis," *Mater Sci Semicond Process*, **135** (2021). doi:10.1016/j.mssp.2021.106096.
101) Y. Feng, Q. Chen, M. Cao, N. Ling, and J. Yao, "Defect-tailoring and titanium substitution in metal-organic framework uio-66-nh2 for the photocatalytic degradation of cr(vi) to cr(iii)," *ACS Appl Nano Mater*, **2** (*9*) 5973–5980 (2019). doi:10.1021/acsanm.9b01403.
102) L. Liu, B. Zhao, D. Wu, X. Wang, W. Yao, Z. Ma, H. Hou, and S. Yu, "Rational design of mof@cof composites with multi-site functional groups for enhanced elimination of u(vi) from aqueous solution," *Chemosphere*, **341** (*September*) 140086 (2023). doi:10.1016/j.chemosphere.2023.140086.
103) S.Z.M. Murtaza, R. Shomal, R. Sabouni, and M. Ghommem, "Facile metal organic framework composites as photocatalysts for lone/simultaneous photodegradation of naproxen, ibuprofen and methyl orange," *Environ Technol Innov*, **27** 102751 (2022). doi:10.1016/j.eti.2022.102751.
104) R. Heu, M. Ateia, C. Yoshimura, D. Awfa, and P. Punyapalakul, "Photocatalytic degradation of organic micropollutants in water by zr-mof/go composites," *Journal of Composites Science*, **4** (*2*) (2020). doi:10.3390/jcs4020054.
105) Y. Zhou, L. Zhou, C. Ni, E. He, L. Yu, and X. Li, "3D/2d mof-derived coceox/g-c3n4 z-scheme heterojunction for visible light photocatalysis: hydrogen production and degradation of carbamazepine," *J Alloys Compd*, **890** 161786 (2022). doi:10.1016/j.jallcom.2021.161786.
106) J. López, A.M. Chávez, A. Rey, and P.M. Álvarez, "Insights into the stability and activity of mil-53(fe) in solar photocatalytic oxidation processes in water," *Catalysts*, **11** (*4*) (2021). doi:10.3390/catal11040448.
107) V.T.T. Nguyen, C.L. Luu, T. Nguyen, A.P. Nguyen, C.T. Hoang, and A.C. Ha, "Multifunctional zn-mof-74 as the gas adsorbent and photocatalyst," *Advances in Natural Sciences: Nanoscience and Nanotechnology*, **11** (*3*) (2020). doi:10.1088/2043-6254/ab9d7c.
108) R.R. Solís, M.A. Quintana, M.Á. Martín-Lara, A. Pérez, M. Calero, and M.J. Muñoz-Batista, "Boosted activity of g-c3n4/uio-66-nh2 heterostructures for the photocatalytic degradation of contaminants in water," *Int J Mol Sci*, **23** (*21*) (2022). doi:10.3390/ijms232112871.

109) W. Wang, Z. Ji, D. Zhang, P. Sun, and J. Duan, "TiO2 doped hkust-1/cm film in the three-phase photocatalytic ammonia synthesis system," *Ceram Int*, **47** (*13*) 19180–19190 (2021). doi:10.1016/j.ceramint.2021.03.265.
110) A. Ray, S.P. Tripathy, S. Dash, S. Subudhi, and K. Parida, "Multivariate co-zn-mof-derived co/c/n-zno nanoflakes decorated with nixpy: a stupefying photocatalyst for pharmaceutical pollutant degradation and hydrogen evolution," *Ind Eng Chem Res*, (2023). doi:10.1021/acs.iecr.3c04178.
111) A. Ray, S. Sultana, L. Paramanik, and K.M. Parida, "Recent advances in phase, size, and morphology-oriented nanostructured nickel phosphide for overall water splitting," *J Mater Chem A Mater*, **8** (*37*) 19196–19245 (2020). doi:10.1039/d0ta05797e.
112) A. Ray, S. Sultana, S.P. Tripathy, and K. Parida, "Aggrandizing the photoactivity of zno nanorods toward n2 reduction and h2 evolution through facile in situ coupling with nixpy," *ACS Sustain Chem Eng*, **9** (*18*) 6305–6317 (2021). doi:10.1021/acssuschemeng.1c00165.
113) A. Ray, S. Subudhi, S.P. Tripathy, L. Acharya, and K. Parida, "MOF derived c/n co-doped zno modified through facile in situ coupling with nixpy toward photocatalytic h2o2 production and h2 evolution reaction," *Adv Mater Interfaces*, **9** (*34*) (2022). doi:10.1002/admi.202201440.
114) P. Behera, A. Ray, S.P. Tripathy, S. Subudhi, L. Acharya, and K. Parida, " Ni x p y cocatalyst-loaded mof-derived c/n–zno@b-doped g-c 3 n 4 -based z-scheme nanohybrid: a combinatorically enhanced ternary photocatalyst towards hydrogen peroxide and hydrogen production ," *ACS Applied Engineering Materials*, **1** (*11*) 2876–2891 (2023). doi:10.1021/acsaenm.3c00403.
115) W. Liu, J. Zhou, D. Liu, S. Liu, X. Liu, S. Xiao, C. Feng, and C. Leng, "Fe-mof by ligand selective pyrolysis for fenton-like process and photocatalysis: accelerating effect of oxygen vacancy," *J Taiwan Inst Chem Eng*, **127** 327–333 (2021). doi:10.1016/j.jtice.2021.08.002.
116) B. Abdollahi, A. Najafidoust, E. Abbasi Asl, and M. Sillanpaa, "Fabrication of zif-8 metal organic framework (mofs)-based cuo-zno photocatalyst with enhanced solar-light-driven property for degradation of organic dyes," *Arabian Journal of Chemistry*, **14** (*12*) (2021). doi:10.1016/j.arabjc.2021.103444.
117) D. Wang, F. Jia, H. Wang, F. Chen, Y. Fang, W. Dong, G. Zeng, X. Li, Q. Yang, and X. Yuan, "Simultaneously efficient adsorption and photocatalytic degradation of tetracycline by fe-based mofs," *J Colloid Interface Sci*, **519** 273–284 (2018). doi:10.1016/j.jcis.2018.02.067.
118) M. Ezaki, and K. Kusakabe, "Highly crystallized tungsten trioxidc loaded titania composites prepared by using ionic liquids and their photocatalytic behaviors," *Evergreen*, **1** (*2*) 18–24 (2014). doi:10.5109/1495159.
119) S. Subudhi, S.P. Tripathy, and K. Parida, "Highlights of the characterization techniques on inorganic, organic (cof) and hybrid (mof) photocatalytic semiconductors," *Catal Sci Technol*, **11** (*2*) 392–415 (2021). doi:10.1039/D0CY02034F.
120) H. Iwakura, H. Einaga, and Y. Teraoka, "Photocatalytic properties of ordered double perovskite oxides," *Kyushu University Global COE Program Journal of Novel Carbon Resource Sciences*, **3** 1–5 (2011).
121) S. Yudha, C. Banon, R. Pertiwi, D.A. Triawan, and J.I. Han, "Cost-effective Synthesis of CeO 2-SiO 2 Based on Oil Palm Leaves for the Removal of Toxic Compounds," 2023.
122) S. Gautam, H. Agrawal, M. Thakur, A. Akbari, H. Sharda, R. Kaur, and M. Amini, "Metal oxides and metal organic frameworks for the photocatalytic degradation: a review," *J Environ Chem Eng*, **8** (*3*) 103726 (2020). doi:10.1016/j.jece.2020.103726.
123) M.S. Khan, Y. Li, D.S. Li, J. Qiu, X. Xu, and H.Y. Yang, "A review of metal-organic framework (mof) materials as an effective photocatalyst for degradation of organic pollutants," *Nanoscale Adv*, 6318–6348 (2023). doi:10.1039/d3na00627a.
124) C. Liu, H. Liu, J.C. Yu, L. Wu, and Z. Li, "Strategies to engineer metal-organic frameworks for efficient photocatalysis," *Chinese Journal of Catalysis*, **55** 1–19 (2023). doi:10.1016/S1872-2067(23)64556-5.
125) D. Jiang, P. Xu, H. Wang, G. Zeng, D. Huang, M. Chen, C. Lai, C. Zhang, J. Wan, and W. Xue, "Strategies to improve metal organic frameworks photocatalyst's performance for degradation of organic pollutants," *Coord Chem Rev*, **376** 449–466 (2018). doi:10.1016/j.ccr.2018.08.005.
126) A. Bhattacharyya, M. Gutiérrez, B. Cohen, A. Valverde-González, M. Iglesias, and A. Douhal, "How does the metal doping in mixed metal mofs influence their photodynamics? a direct evidence for improved photocatalysts," *Mater Today Energy*, **29** (2022). doi:10.1016/j.mtener.2022.101125.
127) C. Brahmi, M. Benltifa, C. Vaulot, L. Michelin, F. Dumur, F. Millange, M. Frigoli, A. Airoudj, F. Morlet-Savary, L. Bousselmi, and J. Lalevée, "New hybrid mof/polymer composites for the photodegradation of organic dyes," *Eur Polym J*, **154** (*May*) (2021). doi:10.1016/j.eurpolymj.2021.110560.
128) S. Rojas, J. García-González, P. Salcedo-Abraira, I. Rincón, J. Castells-Gil, N.M. Padial, C. Marti-Gastaldo, and P. Horcajada, "Ti-based robust mofs in the combined photocatalytic degradation of emerging organic contaminants," *Sci Rep*, **12** (*1*) 1–11 (2022). doi:10.1038/s41598-022-18590-1.
129) I.H. Dwirekso, M. Ibadurrohman, and Slamet, "Synthesis of tio2-sio2-cuo nanocomposite material and its activities for self-cleaning," *Evergreen*, **7** (*2*) 285–291 (2020). doi:10.5109/4055234.
130) P. Behera, S. Subudhi, S.P. Tripathy, and K. Parida, "MOF derived nano-materials: a recent progress in strategic fabrication, characterization and mechanistic insight towards divergent photocatalytic applications," *Coord Chem Rev*, **456** 214392 (2022).

doi:10.1016/j.ccr.2021.214392.
131) L. Pan, T. Muhammad, L. Ma, Z.F. Huang, S. Wang, L. Wang, J.J. Zou, and X. Zhang, "MOF-derived c-doped zno prepared via a two-step calcination for efficient photocatalysis," *Appl Catal B*, **189** 181–191 (2016). doi:10.1016/j.apcatb.2016.02.066.
132) R.M. Rego, G. Kuriya, M.D. Kurkuri, and M. Kigga, "MOF based engineered materials in water remediation: recent trends," *J Hazard Mater*, **403** 123605 (2021). doi:10.1016/J.JHAZMAT.2020.123605.
133) G. Sriram, A. Bendre, E. Mariappan, T. Altalhi, M. Kigga, Y.C. Ching, H.Y. Jung, B. Bhaduri, and M. Kurkuri, "Recent trends in the application of metal-organic frameworks (mofs) for the removal of toxic dyes and their removal mechanism-a review," *Sustainable Materials and Technologies*, **31** e00378 (2022). doi:10.1016/J.SUSMAT.2021.E00378.
134) W. Xiang, Y. Zhang, Y. Chen, C.-J. Liu, and X. Tu, "Synthesis, characterization and application of defective metal-organic frameworks: current status and perspectives," (2020). doi:10.1039/d0ta08009h.